Computational evaluation of inferior vena cava filters through computational fluid dynamics methods

Anand Rajan ⓘ
Mina S. Makary ⓘ
Thomas D. Martyn ⓘ
Joshua D. Dowell ⓘ

ABSTRACT

Numerical simulation is growing in its importance toward the design, testing and evaluation of medical devices. Computational fluid dynamics and finite element analysis allow improved calculation of stress, heat transfer, and flow to better understand the medical device environment. Current research focuses not only on improving medical devices, but also on improving the computational tools themselves. As methods and computer technology allow for faster simulation times, iterations and trials can be performed faster to collect more data. Given the adverse events associated with long-term inferior vena cava (IVC) filter placement, IVC filter design and device evaluation are of paramount importance. This work reviews computational methods used to develop, test, and improve IVC filters to ultimately serve the needs of the patient.

Advanced computing technology increasingly allows the expeditious calculation of solutions to complex problems. Three-dimensional (3D) finite element modeling and computational fluid dynamics, although historically time consuming and expensive, are becoming more accessible and thus more frequently utilized in improving medical devices (1).

Finite element analysis (FEA) involves first modeling the system being analyzed with discrete elements, each of which allows for the variable being studied (e.g., stress, temperature, flow) to be approximated within its domain. After modeling is complete, a numerical matrix is assembled, which represents both the properties of the individual elements and the inter-relationships between the surrounding elements. Finally, known constraints on the problem (e.g., internal pressures) are applied as boundary conditions, and numerical techniques are used to solve the system of equations represented by the matrix. This solution leads to an approximation of the variable being studied (Fig. 1). This method is particularly useful for finding solutions in complex geometries for which closed-form solutions may not exist. Computational fluid dynamics (CFD) is a similar numerical technique used to estimate the behavior of fluids in complex geometries. CFD can be used to model blood flow through the vasculature and around intravascular devices to aid in decision making (2). Computational methods are typically less time-consuming and more cost-effective than some of the current alternatives to testing medical devices *in vitro*.

Today, 3D simulation is used for designing, positioning, and testing devices (3). One such device is the inferior vena cava (IVC) filter, used to trap emboli from the lower extremities when medical anticoagulation is contraindicated. Complications of IVC filter placement include cava wall perforation, intimal hyperplasia, thrombosis, strut fracture, and embolization. Understanding the dynamic environment that IVC filters are placed in, in a patient-specific manner, could potentially decrease the occurrences of these complications (Fig. 2).

Evaluating credibility of CFD in medical device design

Complex CFD methods have the potential to change how we practice patient centered medicine; however, they must first be shown to accurately reflect the scenarios that they model. The reliability of these methods must be verified before they can be used to affect biomedical design and clinical practice. The American Society of Mechanical Engineers (ASME) recently released the V&V 40, a set of standards that outlines a framework to assess

From the Division of Vascular and Interventional Radiology (A.R., M.S.M.), Department of Radiology, The Ohio State University Wexner Medical Center, Columbus, Ohio, USA; GE Aviation, (T.D.M.), Engineering Division, Lynn, Massachusetts, USA; Northwest Radiology and St. Vincent Health (J.D.D. ✉ *Jdowell@ northwestradiology.com*), Indianapolis, Indiana, USA.

the credibility of computational modeling in medical device modeling applications. Central to this framework is the definition of "model risk" which is a combination of inherent errors within the modeling method as well as the risk that decision-making based on the model can lead to patient harm. The value of a credible model cannot be understated, since decisions leading to patient harm based on these models is proportional to their credibility (4, 5).

The accuracy of different CFD methods within a 3D model has recently been evaluated by comparing the model outputs to a velocity map obtained through particle image velocimetry (PIV). PIV uses motion tracking cameras and lasers to measure the velocities of particles in a fluid as they pass. By fabricating an optically transparent 3D model of the device or vessel being studied, PIV can be used to generate velocity maps that can be compared to the CFD estimates. Hariharan et al. (6) studied the credibility of CFD models in the FDA centrifugal blood pump across different laboratories and found that the variability of PIV measurements across different laboratories was more than 20% despite following a standard protocol, with up to a 35% variability in one particular location within the pump. This variability in measurement was possibly related to differences in particles used, differences in flow patterns, and

flow separation. Malinauskas et al. (7) similarly attempted to compare CFD to PIV in centrifugal pumps and nozzles across laboratories, two benchmark flow geometries commonly used in medical devices. The authors concluded that analyses of flow within even "simple" geometries such as those studied are challenging; 57% of pressure head estimates by CFD were within one standard deviation of the mean measured values. Other studies have developed methods to obtain velocimetry data within a "patient-averaged" or representative infrarenal IVC in order to serve as a comparison point for validation of new data from more complex or patient specific geometries (8, 9). Aycock et al. (10) also demonstrated that simple to moderately complex models can be 3D printed in clear resins, so that their flow patterns can then be evaluated using PIV. These results demonstrate the ongoing effort to establish guidelines in evaluating credibility and validity within these complex theoretical modeling methods.

Predicting IVC filter function

The hemodynamic environment of IVC filters has been studied using CFD models. In an effort to understand the effects of trapped emboli on IVC filter function, Stewart et al. (11) compared CFD models of the Greenfield, Simon Nitinol, and TrapEase filters to PIV studies performed *in vitro* and

found that each filter had different patterns of thrombi capture and hemodynamics. The Simon Nitinol filter's complex design was found to introduce the most hemodynamic disturbance cephalad to the IVC filter position. While the authors state that this hemodynamic disturbance is of unknown clinical significance, they predict that it could lead to increased intimal hyperplasia. The TrapEase filter was found to capture smaller volumes of annular thrombi against the vessel wall that subsequently decreased the wall shear stress patterns. Intimal hyperplasia and decreased hemodynamic clot lysis are posited as the results of low wall shear stress due to recirculating flow patterns and struts that contact larger areas of IVC wall (12).

Using different hemodynamic assumptions, Rhabar et al. (13) used computer modeling to assess the contribution of captured clots to thrombogenesis within IVC filters. Their work explored whether or not captured clots can cause sufficient flow disturbance to increase the potential for thrombogenesis. While clinical data are inconclusive, the presence of stagnant zones around an IVC filter appears to increase the risk of thrombosis. The group concluded that flow disturbances proximal to the filter (downstream from clots) are not significantly different enough to recommend use of one IVC filter design over another

Main points

- Finite element analysis and computational fluid dynamics allow improved calculation of stress, heat transfer, and flow to better understand the medical device environment.

- Complications of IVC filter placement include cava wall perforation, intimal hyperplasia, thrombosis, strut fracture, and embolization. These complications have led to FDA warnings, patient awareness efforts, and increased interest in improved filter designs.

- Understanding the dynamic environment that IVC filters are placed in, in a patient-specific manner, could potentially decrease the occurrences of these complications.

- Computer modeling can be helpful in understanding IVC filter function, design, positioning, as well as filter tilt, considerations for retrieval, and strut perforation.

- Future efforts may allow for patient-specific simulations to determine which filter may best serve a patient and minimize the long-term, filter-related adverse events.
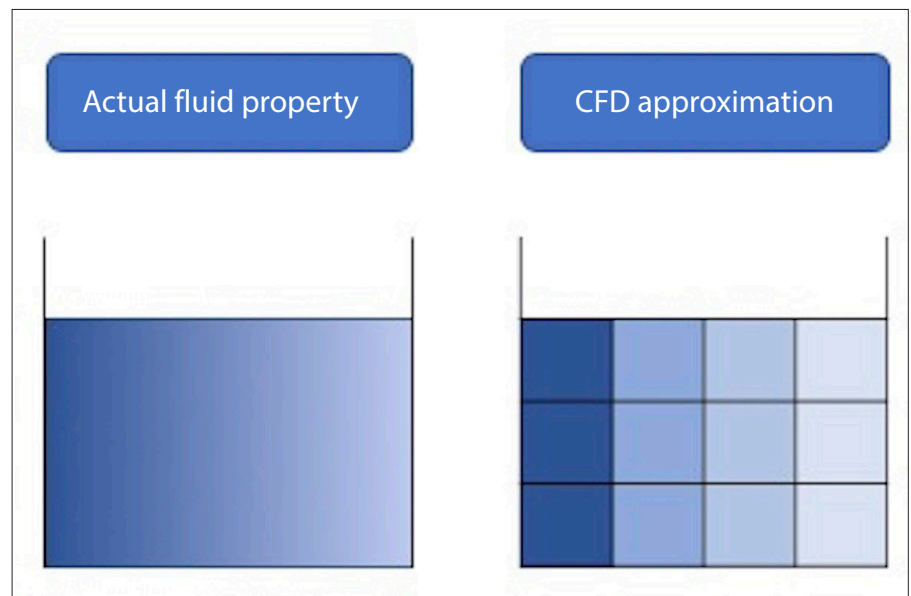
Figure 1. Finite element analysis (FEA) and computational fluid dynamics (CFD) are both used to approximate solutions to problems in physics and engineering by approximating continuous models with discrete points and volumes. As an example of CFD, the image on the left depicts a fluid with a continuously varying property across its volume. The image on the right shows a numeric approximation of this property within finite volumes across the domain.
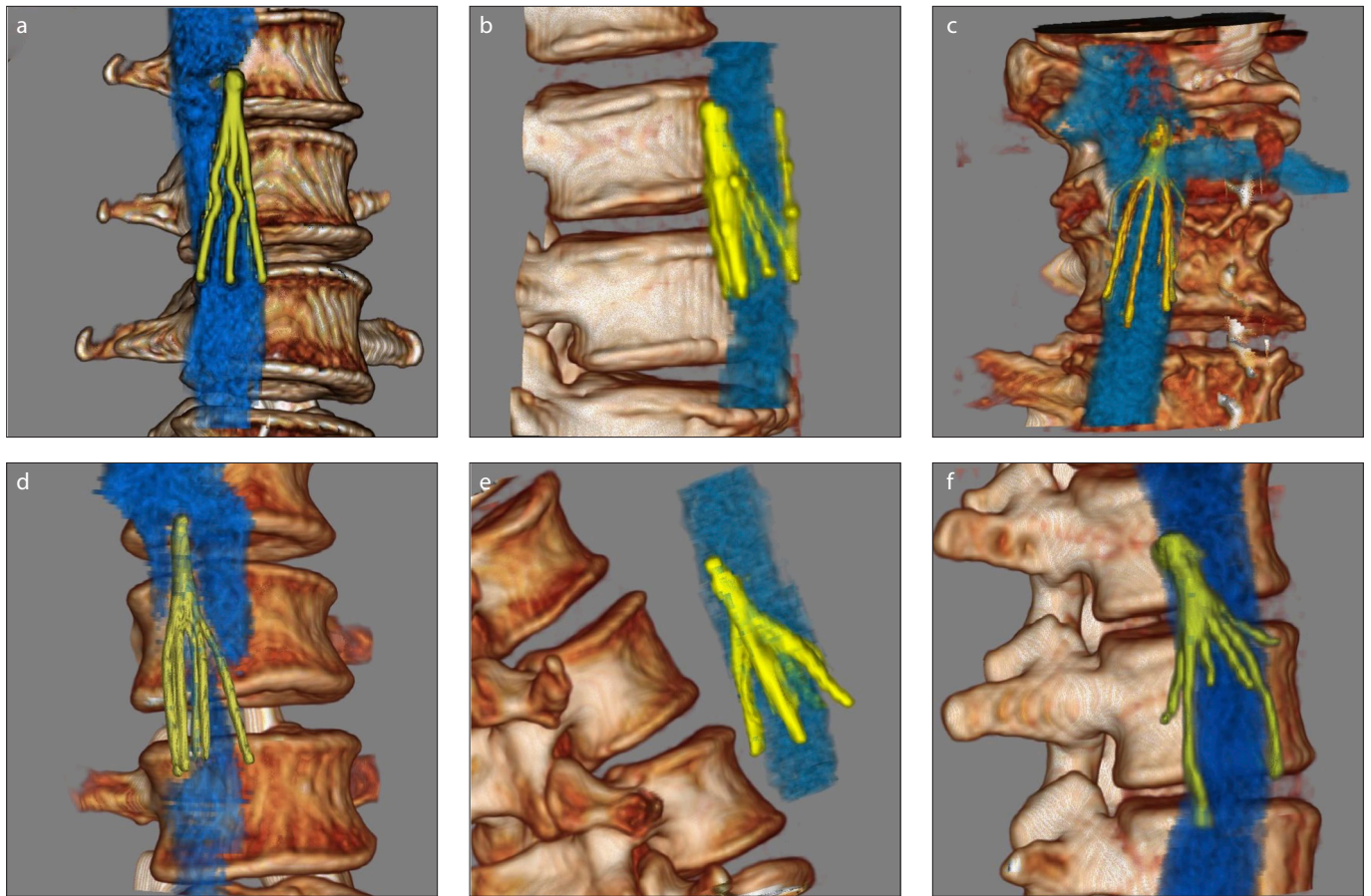
Figure 2. a–f. 3D reconstructions of *in vivo* IVC filters from CT data demonstrating examples of complications. **(a)**, Greenfield (Boston Scientific) filter demonstrating tilt; **(b)**, Vena Tech (B. Braun Medical) filter demonstrating tilt; **(c)**, Denali (Bard Peripheral Vascular) filter demonstrating tilt; **(d)**, Option (Argon Medical Devices) filter demonstrating perforation; **(e)**, Celect (Cook Medical) filter demonstrating tilt and perforation; **(f)**, ALN (Aln International) filter demonstrating tilt and perforation.
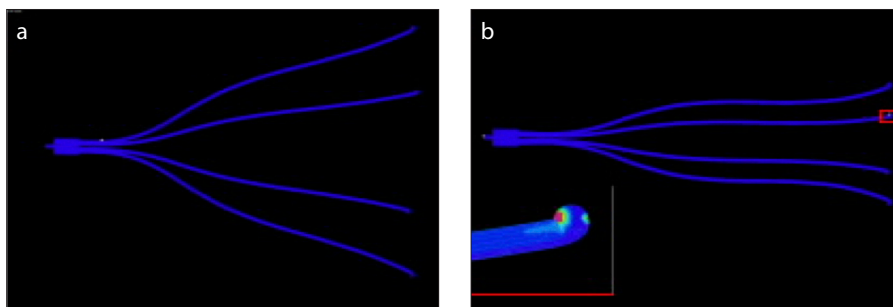

Figure 3. a, b. IVC filter model used by Dowell et al. (36) to evaluate factors contributing to wall perforation by primary struts: **(a)**, IVC filter modeled without load; **(b)**, IVC filter modeled with radial deformation within a 15 mm diameter IVC. Predicted strain on struts represented by color gradient with red areas showing increased strain.

at lower flow rates. However, Ren et al. (14) showed that regions of stagnant and recirculating flow increase with partial occlusion of the IVC and exercise. Regions of stagnant and recirculating flow occur at locations of differences in flow velocity, such as at vein inflow points or around solid bodies within the vessel. Exercise conditions were found to increase the effects of these zones on wall stress. Increased wall stress as a result of these flow disturbances can potentially lead to thrombosis.

The above differences in study results highlight that conclusions drawn from these studies depend highly on the assumptions made and the models used. The use of Newtonian simulations was shown by Aycock et al. (15) to overpredict the Reynolds number and underpredict the wall shear stress (-28% to -54%) calculated by non-Newtonian methods. Across the three IVC models of increasing complexity (straight tube IVC, patient average IVC, Patient specific IVC), non-Newtonian methods showed characteristics of flow that were inherent to more complex patient specific geometry. These methods also had marginally increased computation time and are recommended as the minimum requirement (15). The authors caution that simpler modeling methods may fail to adequately visualize secondary flow patterns that may influence embolus trajectories and effective trapping.

In other studies, Aycock et al. (16, 17) also found positional differences between the embolus trapping capability of the three types of IVC models described previously. Changes in orientation from upright to supine showed variability in embolus trapping capability that was mitigated by secondary flow patterns in the patient-specific IVC. The impact of the morphology of

the IVC on embolus trapping performance suggests that individual variations in patient anatomy must be taken into account separately rather than averaged together. The embolus trapping performance of IVC filters was subsequently shown to increase with embolus size and decrease with filter tilt and trapped emboli load. The clinical relevance of the results of computer modeling studies must thus be explored by further refinement and standardization of modeling methods across the complexity of geometries encountered by the filter *in vivo*.

IVC filter design

Aspects of IVC filter design were examined by Leask et al. (18) to determine the pathogenesis of partial and complete IVC occlusion in patients with a Simon Nitinol IVC filter. Their CFD calculations found a region of low velocity surrounding the apex of the filter that increased when the filter was modeled to be partially occluded. Regions of low velocity correspond to relative stagnant flow zones, and subsequently an increase of the low velocity zone size leads to an increase in the thrombogenic potential proximal to the filter. Singer et al. (19) evaluated the TrapEase filter, which features a dual filter design different from the conical filters mentioned previously. Their CFD calculations again determined regions of decreased velocity that correspond to occlusive and non-occlusive thrombus formation.

Since downstream thrombogenic environments may be exacerbated by trapped emboli, IVC filters could be designed to trap emboli in certain configurations that minimize these downstream effects. Singer et al. (20) explored IVC filter design optimization to minimize hemodynamic effects when partially occluded. Two spherical thrombi were modeled against physiological flow in an IVC and an optimization algorithm was used to position the downstream thrombus to mitigate the negative hemodynamic effects caused by the upstream thrombus. In addition, by elongating the shape of the spherical thrombi along the cava axis, the group was able to further reduce downstream hemodynamic effects (at the cost of increased wall shear stress). This research demonstrates how computer modeling could be used to design filters that trap emboli in optimal configurations and lead to lower rates of occlusion or thrombosis.

IVC filter positioning

Computer modeling can be used to determine effects of different microenvironments on device function. Wang et al. (21) studied the hemodynamic effects of renal vein inflow on the TrapEase and Celect IVC filters. Using CFD methods, they found that nonoccluded or patent filters did not cause a serious downstream disruption cephalad to the filter position to the hemodynamics. Partially occluded filters in the infrarenal position were found to have stagnant flow/recirculating zones cephalad to the filter position that decreased as the filter was moved closer to a juxtarenal position (at the same level as the renal vein inlet). However, partially occluded filters were found to have increased stagnant flow zones when the filter was placed superior to the renal vein inlet, suggesting that this position may result in further thrombosis. The optimal position was thus found to be a near-juxtarenal position upstream of the renal inlet with the apex at the same level as the renal vein inflow, where high velocity inflow might exert a protective effect on the thrombogenic apex region of the filter.

Numerical simulation can be performed on patient-specific models of the IVC to determine optimal filter placement location and performance. Aycock et al. (22) described a computational method to assess IVC filter performance in variant anatomy. The two patient-specific models tested were left-sided IVC and retroaortic IVC. The computer models demonstrated regions of low wall stress at interfaces between IVC filter and IVC in both of the tested anatomies. This low wall stress region was found to be larger in the retroaortic IVC. The left-sided IVC also had a large recirculating flow region with an additional low wall stress region along the left infrarenal IVC wall. These models show how different the microenvironments can be in anatomical variants both pre and post IVC filter placement. By iterating this modeling process with different filter locations, the configuration with the least thrombogenic profile can be deployed, to help reduce complications in patients with atypical IVC anatomy. Recent works of Aycock et al. (9, 15, 16) continue to demonstrate that positioning of IVC filters affects their efficacy in emboli trapping. Further, others have investigated CFD modeling of patient specific and idealized vena cava designs in the presence of different IVC filters to show their effectiveness (23–27).

These models collectively show that complication rates can be further decreased by considering and calculating the exact hemodynamic environment of different filters with respect to the anatomic vasculature of each unique patient.

IVC filter tilt and retrieval

While IVC filter retrieval attempts are highly successful technically in the interventional radiology setting, challenging retrieval procedures and complications can occur. Modeling may serve as a supplement to improve procedural planning and filter retrieval attempts (28, 29). Modeling can further improve our knowledge of a filter position's effect on hemodynamics by exploring the consequences of an off-center IVC filter. A tilted IVC filter can function suboptimally and often presents a challenge to retrieval. Singer et al. (30) showed through computer modeling that tilt may additionally increase the potential for thrombogenesis in patients with permanent filters demonstrating significant tilt. They studied the impact of filter tilt on the hemodynamic environment within the IVC. Their computer models found that tilted IVC filters produced a stagnant zone between the filter apex and the vessel wall. The stagnant zone was found to become larger when the filter tip was modeled closer to the vessel wall. Stagnant flow zones were also found to extend above the filter position when the filter (and thus IVC) was modeled as completely occluded with a spherical thrombus.

In addition to thrombosis, tilted filters can also complicate filter retrieval. Dowell et al. (31) compared retrieval of two conical IVC filter designs, namely the Argon Option and Bard Denali IVC filters. Despite their similar designs, the Argon Option IVC filter required advanced retrieval significantly more often than the Bard Denali filter, possibly as a result of increased cava wall remodeling when the Argon Option is used. Tilted filters that require advanced retrieval have also been shown to result in a significant increase in fluoroscopy time (32). Computer modeling allows a method to better understand the impact of tilt and procedural planning ahead of a challenging retrieval.

IVC filter perforation

Perforation of the IVC wall after filter placement is related to normal (perpendicular) and shear (parallel) forces on the filter surfaces, long-term placement, and chang-

es in the IVC walls as a result of malignancy. Hernández and Peña (33) quantified the failure properties of the IVC with respect to normal force related fracture using *in vitro* IVC models harvested from sheep; however, *in vitro* examinations of shear stress related IVC perforation are scarce. Pérez-Andrés and Peña (34) developed a method to analyze filter perforation related to deployment of filters using the data on normal force related IVC fracture and determined that penetration does not occur due to filter deployment. They suggest that other physiologic mechanisms such as respiratory variation of IVC size and Valsalva maneuver are likely to be larger contributors to the perforation phenomenon. Variations in IVC cross-sectional area secondary to Valsalva maneuver are in fact shown by Laborda et al. (35) to be strongly related to IVC filter penetration due to radial forces.

Dowell et al. (36) used finite element analysis to study the effects of IVC size and shape on strut deformation and subsequent risk of perforation for the Cook Celect IVC filter. They found that smaller IVC diameters resulted in higher strut normal and total forces (Fig. 3). Once a threshold force was reached by the IVC filter strut against the IVC wall, strut perforation would follow. Their models suggested that filter-related perforations might occur more frequently in women and those with malignancy due to a lower average strut force required for perforation.

After establishing higher filter strut forces within IVCs with ellipse cross-section, they modeled strut forces from sequential CT studies in representative patients that demonstrated progressive strut perforation over time. Their model demonstrated redistributed forces on the adjacent strut feet following an initial strut perforation. This model allowed the prediction of additional strut perforation by estimating the force threshold necessary for a second perforation by another strut following an initial perforation. While there is continued incidence of IVC filter perforation without symptomatic complications in the population, research into this area could further improve complication rates. Computer modeling may therefore help predict elements of a device that might be more prone to failure.

Conclusion and future directions

As technology continues to evolve, processor performance will continue to grow and multi-physics (structural, heat transfer, fluid) numerical simulation will become quicker, more accurate, and more accessible. Limitations do exist to CFD in modeling the IVC environment as described above. The methods themselves must hold up to scrutiny, and credibility evaluations such as the V&V 40 will be instrumental in holding CFD to a high standard for patient care decision making. The complexity of patient-specific IVC geometries require more complex non-Newtonian calculations to adequately capture secondary flow zones, and a deep understanding of hemorheology is required to ensure the models represent states as close to *in vivo* states as possible. Additionally, modeling the physical characteristics of IVC filters represents a unique challenge as they are made of Nitinol, a memory metal with the unique characteristic of "remembering" its deployed shape. Limitations will continue to exist in modeling the IVC as a dynamic structure that responds to physiologic maneuvers, rather than a static tube. As knowledge on theoretical aspects of heat transfer, fluid dynamics, and vascular microenvironments continues to grow, computer models will become more sophisticated, possibly leading to improved evaluation of medical devices and prediction of their shortcomings.

As demonstrated, positioning of IVC filters has important implications for optimal function. Improved understanding of IVC filter characteristics by computer modeling may aid in IVC filter design to incorporate the advantages of the IVC filters available today while minimizing their long-term complications. By understanding a patient's anatomy prior to filter placement, modeling may allow patient-specific simulations to determine which filter may best serve a patient and minimize the long-term, filter-related adverse events. The future of computer modeling and simulation in medical device design, development, and testing continues to be promising.

Conflict of interest disclosure
The authors declared no conflicts of interest.

References
1. Zarins CK, Taylor CA. Endovascular device design in the future: transformation from trial and error to computational design. J Endovasc Ther 2009; 16 Suppl 1:I12–21. [Crossref]
2. Itatani K, Miyazaki S, Furusawa T, et al. New imaging tools in cardiovascular medicine: computational fluid dynamics and 4D flow MRI. Gen Thorac Cardiovasc Surg 2017; 65:611–621. [Crossref]
3. Petrini L, Trotta A, Dordoni E, et al. A computational approach for the prediction of fatigue behaviour in peripheral stents: application to a clinical case. Ann Biomed Eng 2016; 44:536–547. [Crossref]
4. Assessing credibility of computational modeling through verification and validation: Application to medical devices V&V Standard 40. ASME, 2018.
5. Morrison TM, Hariharan P, Funkhouser CM, Afshari P, Goodin M, Horner M. Assessing computational model credibility using a risk-based framework: application to hemolysis in centrifugal blood pumps. ASAIO J 2019; 65:349–360. [Crossref]
6. Hariharan P, Aycock KI, Buesen M, et al. Inter-laboratory characterization of the velocity field in the FDA blood pump model using particle image velocimetry (PIV). Cardiovasc Eng Technol 2018; 9:623–640. [Crossref]
7. Malinauskas RA, Hariharan P, Day SW, et al. FDA benchmark medical device flow models for CFD validation. ASAIO J 2017; 63:150–160. [Crossref]
8. Gallagher MB, Aycock KI, Craven BA, Manning KB. Steady flow in a patient-averaged inferior vena cava—Part I: Particle image velocimetry measurements at rest and exercise conditions. Cardiovasc Eng Technol 2018; 9:641–653. [Crossref]
9. Craven BA, Aycock KI, Manning KB. Steady flow in a patient-averaged inferior vena cava—Part II: Computational fluid dynamics verification and validation. Cardiovasc Eng Technol 2018; 9:654–673. [Crossref]
10. Aycock KI, Hariharan P, Craven BA. Particle image velocimetry measurements in an anatomical vascular model fabricated using inkjet 3D printing. Experiments Fluids 2017; 58:154. [Crossref]
11. Stewart SF, Robinson RA, Nelson RA, Malinauskas RA. Effects of thrombosed vena cava filters on blood flow: flow visualization and numerical modeling. Ann Biomed Eng 2008; 36:1764–1781. [Crossref]
12. Nicolás M, Peña E, Malvè M, Martínez MA. Mathematical modeling of the fibrosis process in the implantation of inferior vena cava filters. J Theor Biol 2015; 387:228–240. [Crossref]
13. Rahbar E, Mori D, Moore JE. Three-dimensional analysis of flow disturbances caused by clots in inferior vena cava filters. J Vasc Interv Radiol 2011; 22:835–842. [Crossref]
14. Ren Z, Wang SL, Singer MA. Modeling hemodynamics in an unoccluded and partially occluded inferior vena cava under rest and exercise conditions. Med Biol Eng Comput 2012; 50:277–287. [Crossref]
15. Aycock KI, Campbell RL, Lynch FC, Manning KB, Craven, BA. The importance of hemorheology and patient anatomy on the hemodynamics in the inferior vena cava. Ann Biomed Eng 2016; 44:3568–3582. [Crossref]
16. Aycock KI, Campbell RL, Lynch FC, Manning KB, Craven BA. Computational predictions of the embolus-trapping performance of an IVC filter in patient-specific and idealized IVC geometries. Biomech Model Mechanobiol 2017; 16:1957–1969. [Crossref]
17. Aycock KI, Campbell RL, Manning KB, Craven BA. A resolved two-way coupled CFD/6-DOF approach for predicting embolus transport and the embolus-trapping efficiency of IVC filters. Biomech Model Mechanobiol 2017; 16:851–869. [Crossref]

18. Leask RL, Johnston KW, Ojha M. In vitro hemodynamic evaluation of a Simon nitinol vena cava filter: possible explanation of IVC occlusion. J Vasc Interv Radiol 2001; 12:613–618. [Crossref]

19. Singer MA, Henshaw WD, Wang SL. Computational modeling of blood flow in the TrapEase inferior vena cava filter. J Vasc Interv Radiol 2009; 20:799–805. [Crossref]

20. Singer MA, Wang SL, Diachin DP. Design optimization of vena cava filters: an application to dual filtration devices. J Biomech Eng 2010; 132:101006. [Crossref]

21. Wang SL, Singer MA. Toward an optimal position for inferior vena cava filters: computational modeling of the impact of renal vein inflow with Celect and TrapEase filters. J Vasc Interv Radiol 2010; 21:367–374. [Crossref]

22. Aycock KI, Campbell RL, Manning KB, et al. A computational method for predicting inferior vena cava filter performance on a patient-specific basis. J Biomech Eng 2014; 136:10.1115/1.4027612. [Crossref]

23. Nicolas M, Malve M, Pena E, Martinez MA, Leask R. In vitro comparison of Gunther Tulip and Celect filters. Testing filtering efficiency and pressure drop. J Biomechanics 2015; 48:504–511. [Crossref]

24. Nicolas M, Palero VR, Pena E, et al. Numerical and experimental study of the fluid flow through a medical device. Int Comm Heat Mass Transfer 2015; 61:170–178. [Crossref]

25. Lopez JM, Fortuny G, Puigjaner D, Herrero J, Marimon E. A comparative CFD study of four inferior vena cava filters. Int J Numer Method Biomed Eng 2018; 34:e2990. [Crossref]

26. Laborda A, Sierre S, Malve M, et al. Influence of breathing movements and Valsalva maneuver on vena caval dynamics. World J Radiol 2014; 6:833–839. [Crossref]

27. Tedaldi E, Montanari C, Aycock KI, et al. An experimental and computational study of the inferior vena cava hemodynamics under respiratory-induced collapse of the infrarenal IVC. Med Eng Phys 2018; 54:44–55. [Crossref]

28. Makary MS, Kapke J, Yildiz V, Pan X, Dowell JD. Outcomes and direct costs of inferior vena cava filter placement and retrieval within the IR and surgical settings. J Vasc Interv Radiol 2018; 29:170–175. [Crossref]

29. Makary MS, Shah SH, Warhadpande S, Vargas IG, Sarbinoff J, Dowell JD. Design-of-experiments approach to improving inferior vena cava filter retrieval rates. J Am Coll Radiol 2017; 14:72–77. [Crossref]

30. Singer MA, Wang SL. Modeling blood flow in a tilted inferior vena cava filter: does tilt adversely affect hemodynamics? J Vasc Interv Radiol 2011; 22:229–235. [Crossref]

31. Dowell JD, Semaan D, Makary MS, Ryu J, Khayat M, Pan X. Retrieval characteristics of the Bard Denali and Argon Option inferior vena cava filters. J Vasc Surg Venous Lymphat Disord 2017; 5:800–804. [Crossref]

32. Dowell JD, Wagner D, Elliott E, Yildiz VO, Pan X. Factors associated with advanced inferior vena cava filter removals: a single-center retrospective study of 203 patients over 7 years. Cardiovasc Intervent Radiol 2016; 39:218–226. [Crossref]

33. Hernández Q, Peña E. Failure properties of vena cava tissue due to deep penetration during filter insertion. Biomech Model Mechanobiol 2016; 15:845–856. [Crossref]

34. Pérez-Andrés A, Peña E. Calibration of interface properties and application to a finite element model for predicting vena cava filter-induced vein wall failure. Int J Num Methods Biomed Eng 2018; 34:e3098. [Crossref]

35. Laborda A, Kuo WT, Ioakeim I, et al. Respiratory-induced haemodynamic changes: a contributing factor to IVC filter penetration. Cardiovasc Intervent Radiol 2015; 38:1192–1197. [Crossref]

36. Dowell JD, Castle JC, Schickel M, et al. Celect inferior vena cava wall strut perforation begets additional strut perforation. J Vasc Interv Radiol 2015; 26:1510–1518.e3. [Crossref]